CHEMISTRY
A EUROPEAN JOURNAL

DOI: 10.1002/chem.200800803

Morphological Transformation of $Co(OH)_2$ Microspheres from Solid to Flowerlike Hollow Core–Shell Structures

Ru Qiao,[a] Xiao Li Zhang,[c] Ri Qiu,[a] Ju Chang Kim,[a] and Young Soo Kang*[b]

Abstract: We report, for the first time, a detailed investigation into the formation of highly uniform, 3D, flowerlike, hollow, spherical architectures of cobalt hydroxide through a facile solvothermal process. Various controlling parameters were examined, such as water content in starting materials, reaction time, cobalt(II) precursor concentration, and reaction temperature. On the basis of the experimental results, the formation mechanism of these flowerlike cobalt hydroxide hollow spheres involves aggregation of cobalt hydroxide building clusters into solid spheres and hollowing effect through subsequent dissolution, diffusion, and re-deposition of the smaller crystallites under the surface layer driven by an Ostwald ripening process. Metallic cobalt hollow spheres have also been obtained by thermal decomposition of cobalt hydroxide flowers in a mixed gas of Ar+4% H_2 at 400 °C. The morphology and composition of the products were characterized by X-ray diffraction, field-emission scanning electron microscopy, energy-dispersive X-ray spectroscopy, and (high resolution) transmission electron microscopy.

Keywords: cobalt · materials science · nanostructures · Ostwald ripening · solvothermal process

Introduction

Divalent transition-metal hydroxides, cobalt hydroxides, have been extensively studied over the last two decades, owing to their unique physico-chemical properties for electrochemical, magnetic, and catalytic applications. As reported by Li et al., cobalt hydroxide can be used as additives in nickel hydroxide electrode to improve high-temperature and high-rate discharge ability beneficially.[1] The composite material of cobalt hydroxide on ultra-stable Y zeolite molecular sieves shows a potential application as a novel electrochemical capacitor with high energy density.[2] Electrodeposited cobalt hydroxide films show eletrocatalytic properties for urea oxidation and methanol oxidation in alkaline solution.[3] Kurmoo reported the synthesis of hard magnets based on layered cobalt hydroxides that incorporate anionic surfactants,[4] and the interlayer spacings were tunable through electrodeposition by incorporating long-chain surfactant molecules into the interlayer regions.[5]

It is well known that cobalt hydroxide can be crystallized into a hexagonal layered structure with two polymorphic forms, α- and β-$Co(OH)_2$. These β-hydroxides are composed of $Co(OH)_2$ with a brucite-like structure, which consists of the hexagonal packing of hydroxyl ions, with Co^{II} occupying alternate rows of octahedral sites,[6] and exhibits a characteristic pink color, whereas α phases are isostructural with hydrotalcite-like compounds that consists of stacked $Co(OH)_{2-x}$ layers intercalated with various anions (e.g. nitrate, carbonate, etc.) in the interlayer space to restore charge neutrality,[6] and their color also change from pink to green/blue. Thus, α-$Co(OH)_2$ has a larger layer spacing than the brucite-like β-$Co(OH)_2$ so that α form has higher electrochemical activity. However, this hydrotalcite-like phase is metastable and easily transforms into more stable brucite-like compounds in strongly alkaline media. Accordingly, β-$Co(OH)_2$ is often selected as additives of alkaline secondary batteries owing to its stability and enhanced conductivity when changed to β-CoOOH.

The preparation of single-crystal $Co(OH)_2$ hexagonal micro- and nanoflakes is easily achieved by solution meth-

[a] Dr. R. Qiao, R. Qiu, Prof. J. C. Kim
Department of Chemistry, Pukyong National University
599–1 Daeyeon-3-dong, Namgu
Busan 608–737 (South Korea)
[b] Prof. Y. S. Kang
Department of Chemistry, Sogang University
#1 Shinsu-dong, Mapo-gu
Seoul 121–742 (South Korea)
Fax: (+82)-2-701-0967
E-mail: yskang@sogang.ac.kr
[c] Dr. X. L. Zhang
ARC Center of Electromaterials Science
Department of Materials Engineering, Monash University
Clayton VIC (Australia)

ods and has been much demonstrated because of their intrinsic layered crystal structure.[7] Among them, the hydrolysis of Co^{2+} ions absorbed in a multilayered polymer network to form cobalt hydroxide nanocrystals reported by Zhang et al. is very interesting and worthy of attention.[8] Their studies suggest that the formation of needlelike α-$Co(OH)_2$ and hexagonal β-$Co(OH)_2$ can be controlled by varying the reaction environment from nitrogen to oxygen. Nanorod,[7g,9] nanosheet,[9b] and nanoneedle[10] morphologies have also been reported, whereas, there are few reports on the formation of 3D $Co(OH)_2$ architectures assembled from nanostructures. Zeng's group reported the synthesis of butterfly-like β-$Co(OH)_2$ nanocrystallites with the assistance of chelating agent ethylenediamine.[7g] Xie and co-workers synthesized sisal-like, dandelion-like, and rose-like $Co(OH)_2$ architectures by aggregation of well-arranged nanorods and nanoflakes.[11] Yang et al. also reported the preparation of β-$Co(OH)_2$ carnation-like aggregation assembled by nanosheets to reduce the surface energy.[12] At present, the preparation of $Co(OH)_2$ 3D hierarchical structures is still a big challenge and attraction for researchers.

In this study we report our recent efforts on the synthesis of 3D flowerlike β-$Co(OH)_2$ microspheres with hollow interiors on a large scale through a facile selected-control solvothermal process, without templates in the reaction system. Analysis of a series of time-dependent experiments that utilized field-emission scanning electron microscopy (FESEM), transmission electron microscopy (TEM) and X-ray diffraction (XRD), reveals that these flowerlike $Co(OH)_2$ spheres are obtained by self-transformation from solid to hollow core–shell structure after a reaction time of about 8 h. This transformation proceeds under the driving force of Ostwald ripening process in which larger crystal particles are essentially immobile and keep growing, while smaller ones are undergoing mass relocation through dissolving and regrowing.[13] In addition to examining the effects of reaction time on the morphological control we also studied other synthetic parameters, such as water content, cobalt(II) precursor concentration, and reaction temperature. There are two significant features in this work: First, this is the first report of flowerlike hollow core–shell architectures of cobalt hydroxide, and second, this synthesis process used to prepare hollow spherical structures in neither template-directed method nor an emulsion method, is simple and easy-manipulated. The corresponding metallic cobalt hollow spheres were readily obtained by thermal decomposition of $Co(OH)_2$ hollow flowers in mixed gas of Ar+4% H_2.

Results and Discussion

Flowerlike β-$Co(OH)_2$ hollow microspheres were prepared under mild solvothermal conditions in a solution containing $CoCl_2{\cdot}6H_2O$, ethylene glycol (EG), NaOH, and distilled water (see Sample 1 in Table 1 for details). The product obtained after heating at 200 °C for 8 h consists of a high yield of flowerlike hollow microspheres 4 ± 0.5 μm in size (Figure 1a). The high-magnification field-emission scanning electron microscopy (FESEM) image (Figure 1b) shows that the shell of individual microspheres is approximately 0.8–1.0 μm in uniform thickness, and the external surface of the shell wall consists of numerous randomly packed nanoflakes with a radial form (inset of Figure 1b). The phase of the as-prepared sample was identified by XRD measurement, and the XRD pattern of the final pink product is shown in Figure 2a. It exhibits a brucite-like phase (JCPDS file no. 30-0443) in which the 2θ scan has peaks at 32.9°, 37.6°, and 58.0°, corresponding to the (100), (101), and (110) diffraction. Meanwhile, there are two peaks at 35.8° and 42.0° correspond to (111) and (200) diffraction of the CoO phase (JCPDS file

Table 1. Detailed experimental parameters for the synthesis of typical samples and their morphologies.

Sample	Reaction system	t [h]	T [°C]	Morphology
1	2 mmol $CoCl_2{\cdot}6H_2O$+ 2.5 mmol NaOH+0.1 mL H_2O+39.9 mL EG	8	200 °C	flowerlike hollow spheres
2	2 mmol $CoCl_2{\cdot}6H_2O$+ 2.5 mmol NaOH+0.2 mL H_2O+39.8 mL EG	8	200 °C	nanoflakes and flowerlike aggregations
3	1 mmol $CoCl_2{\cdot}6H_2O$, other terms same as Sample 1	8	200 °C	nanoflakes and solid Co spheres
4	3 mmol $CoCl_2{\cdot}6H_2O$, other terms same as Sample 1	8	200 °C	hexagonal aggregations by nanoplates
5	same as Sample 1	3	200 °C	solid spheres
6	same as Sample 1	4	200 °C	flowerlike core–shell structures
7	same as Sample 1	8	180 °C	flowerlike core–shell structures
8	same as Sample 1	8	220 °C	flowerlike hollow spheres

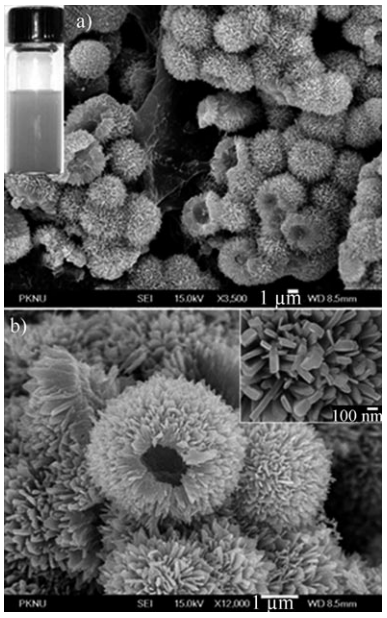

Figure 1. a) Low- and b) high-magnification FESEM images of flowerlike hollow spheres of β-$Co(OH)_2$ obtained from Sample 1. Insets of a) and b) show β-$Co(OH)_2$ suspension by dispersing the product in ethanol and surface structure, respectively.

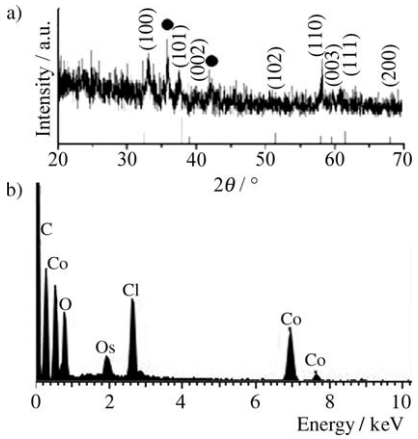

Figure 2. a) The XRD pattern and b) EDS spectrum obtained from the flowerlike $Co(OH)_2$ hollow spheres (Sample 1).

no. 09-0402), which was obtained by thermal decomposition of a few of cobalt hydroxides: $Co(OH)_2 \rightarrow CoO + H_2O$. EDS measurement reveals a homogeneous distribution of elements in the sample (Figure 2b). Os signal comes from the Os film which was coated onto the sample for FESEM observation to prevent negative charge build-up on the sample, and the appearance of Cl signal is caused by the adsorption of Cl^- anions.

In this reaction system, it is believed that water content in the mixed solvent has a great influence on the morphology of the product. Hollow flowers could be obtained by using a V_W/V_{EG} ratio of 0.1:39.9 (V_w= volume of water, V_{EG}= volume of ethylene glycol). If the V_W/V_{EG} ratio was adjusted to 0.2:39.8 (Sample 2), β-$Co(OH)_2$ nanoflakes were obtained and could form irregular flowerlike aggregates to decrease the high surface energy in the high-concentration areas (Figure 3a). Upon increasing the V_W/V_{EG} ratio to 0.5:39.5, 1:39, and 10:30, we could get nanoflakes with a larger width and length, which seldom aggregated (Figure 3b–d). It indicates that $Co(OH)_2$ crystals prefer to grow into nanoflakes, as a result of their intrinsic lamellar structures rather than aggregate to form spherical structures, when the viscosity of the EG/water solvent decreases with increasing water content.

We also studied the effect of cobalt chloride concentration on the products, with a constant V_W/V_{EG} ratio of 0.1:39.9. When the amount of cobalt chloride was decreased to 1 mmol, a mixture of β-$Co(OH)_2$ nanoflakes and metallic Co spheres was obtained (Sample 3, Figure 4a). They were separated by a magnet and characterized by FESEM and TEM. Two separated morphologies of Co spheres and $Co(OH)_2$ nanoflakes, respectively, are shown in Figure b,c. The 2θ scan of the XRD pattern has a peak at 44.5° to correspond to the (111) diffraction of Co cubic structure (JCPDS file no. 01-1259), thus confirming that EG can act as a weak reducing agent to reduce Co^{2+} (in $Co(OH)_2$) to Co^0 (in Co) in alkaline media at high temperature. However, if more cobalt chloride (3 mmol, Sample 4) was used, the product contained single phase of β-$Co(OH)_2$, which had a pink color. As shown in Figure 5, the product morphology

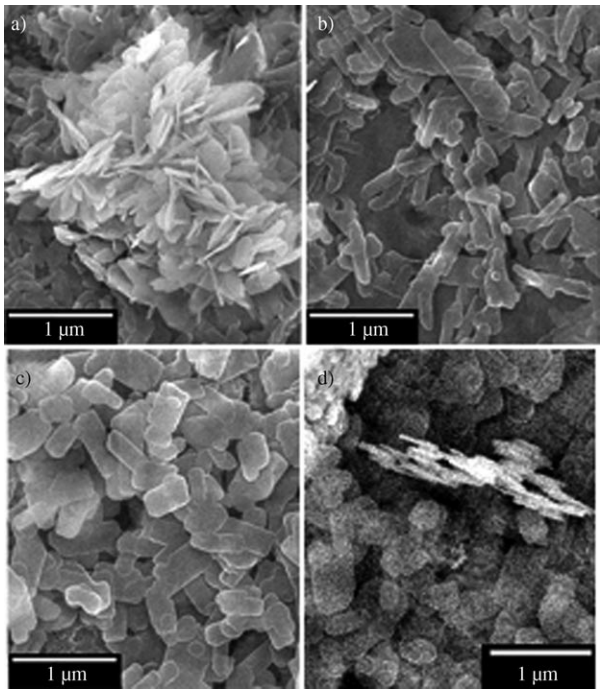

Figure 3. a) FESEM image of flowerlike aggregation of $Co(OH)_2$ nanoflakes obtained by adjusting V_W/V_{EG} to 0.2:39.8 (Sample 2). b,c) FESEM images of $Co(OH)_2$ nanoflakes obtained by increasing V_W/V_{EG} to 0.5:39.5 and 1:39, respectively. d) FESEM image of $Co(OH)_2$ nanoflakes obtained by increasing V_W/V_{EG} to 10:30.

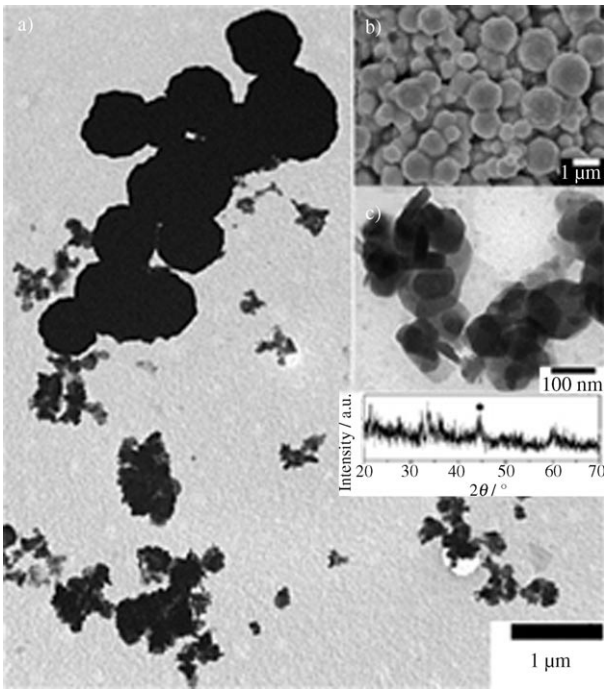

Figure 4. a) TEM image of a mixture of β-$Co(OH)_2$ nanoflakes and Co microspheres obtained by adjusting $CoCl_2$ to 1 mmol (Sample 3). Inset of a) XRD pattern of this mixture. b,c) FESEM and TEM images of Co microspheres and $Co(OH)_2$ nanoflakes obtained by separation, respectively.

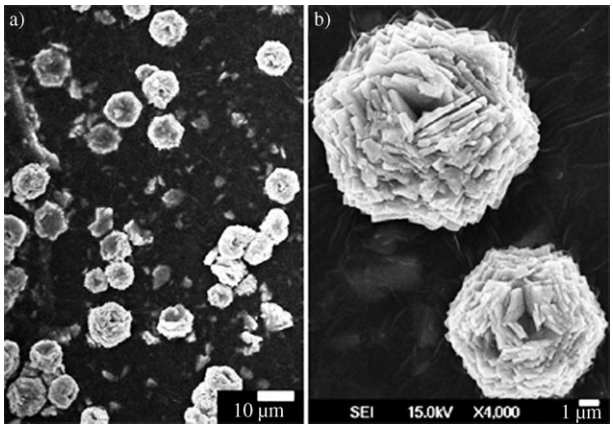

Figure 5. a) Low- and b) high-magnification FESEM images of hexagonal aggregation of nanoplates obtained by adjusting $CoCl_2$ to 3 mmol (Sample 4).

was hexagonal aggregation of nanoplates. Figure 5b shows a high-magnification FESEM image of such a single structure. This hexagonal aggregation is a layered assembly of numerous nanoplates. These plates are arranged at progressively increasing angles to the radial axis and highly directed to form arrays in the regular fashion, which also results in a concave central part and minimizes the total-surface energy by reducing exposed areas.

To further investigate the formation process of flowerlike $Co(OH)_2$ microspheres with hollow interiors, the intermediate products with different precipitation durations were studied in detail by TEM, FESEM, and XRD analysis of structures isolated from the reaction mixture maintained at 200 °C. Figure 6 shows detailed time-dependent evolutions of morphology and crystallinity. A sample obtained after 1.5 h of reaction, which contains nanosized colloidal particles, can be seen in Figure 6a. When the reaction time was prolonged to 3 h (Sample 5), as shown in Figure 6b and inset, a high yield of solid microspheres with diameters of about 2 μm grew from the nanosized colloidal spheres. After 4 h of reaction, the diameters increased to about 3 μm, and it was also found that small surface flakes formed shells on the solid cores, creating a core-shell structure (Figure 6c, Sample 6). Interestingly, these cores shrunk over time to form a sphere-in-sphere structure,[14] which had a continu-

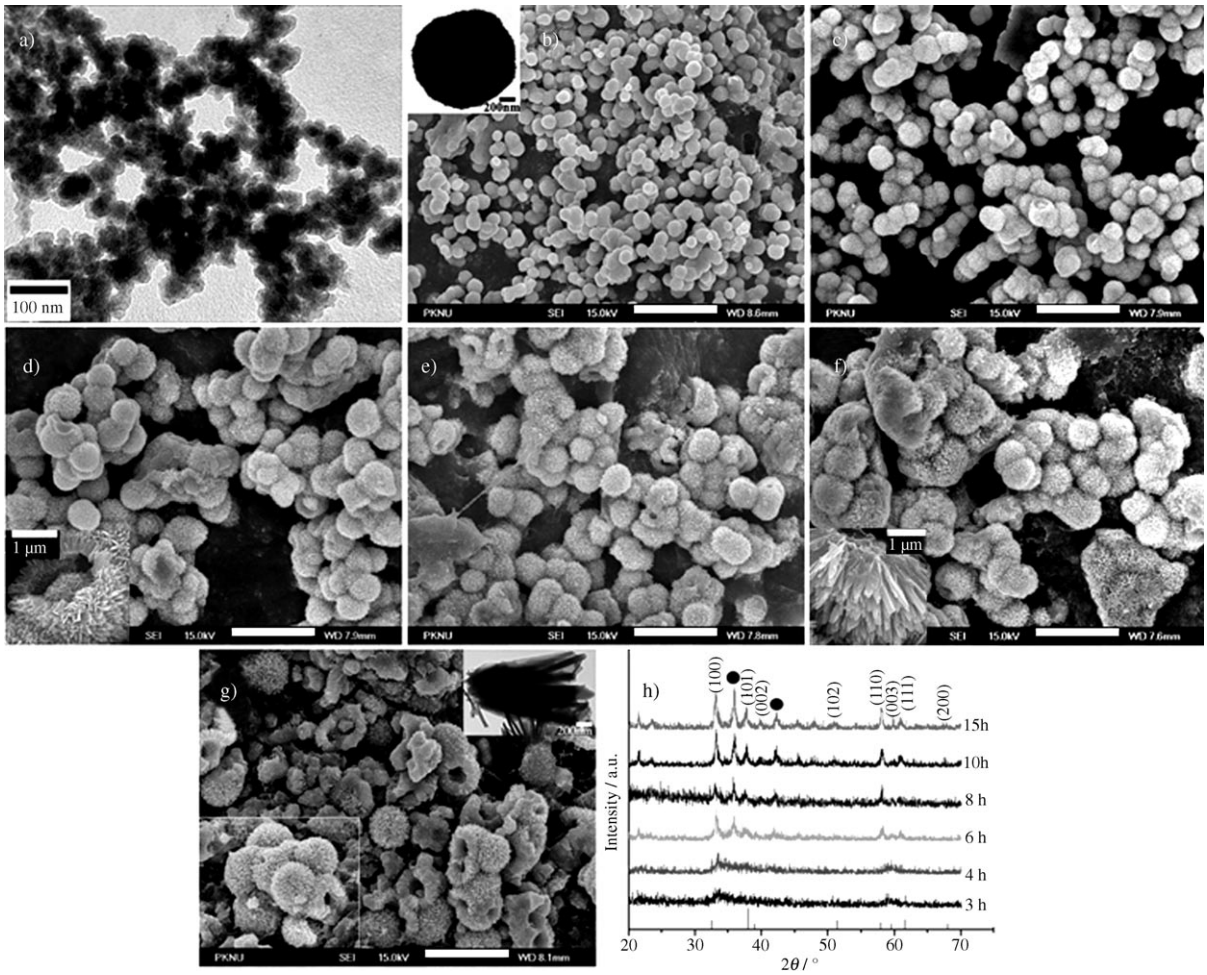

Figure 6. TEM and FESEM (insets) images of the cobalt hydroxide spheres prepared for a) 1.5, b) 3, c) 4, d) 6, e) 8, f) 10, and g) 15 h, showing morphological transformation from self-aggregation to solid spheres, and then to hollow flowers. h) XRD patterns of products obtained from different reaction stages. The scale bars shown in b)–g) are all 10 μm.

ously reducing innersphere size (Figure 6d). From the high magnification image of individual broken sphere (inset of Figure 6d), it can be seen clearly that interior void between core and shell has increased. The innerspheres disappeared completely after 8 h of reaction and created a hollow core structure (Figure 1 and Figure 6e). The nanoflakes grew further over time to form a flowerlike prickly surface. If the reaction time was prolonged further to 10 h and 15 h, the outside-sphere diameters also increased to 4.2 μm and 5.2 μm, respectively (Figure 6f, g). XRD patterns of the samples obtained at different stages (Figure 6h) display the gradual increase of the crystallinity of β-$Co(OH)_2$ products. By using the Scherrer–Debye formula for an estimation of progressive crystallite growth, we found that the size of the crystallite formed in this process was increased from 10.5 to 35.1 nm.

It is clear that the growth process is neither surfactant-assisted nor template-directed for the formation mechanism of the flowerlike β-$Co(OH)_2$ hollow microspheres, because no surfactants or templates were used in the reaction system. On the basis of the above evaluation of the time-dependent morphology and crystallinity, it is believed that Ostwald ripening process should be the main driving force for these transformations. This process is associated with a progressive redistribution of matter from the interior to exterior of the microspheres. The formation process of the hollow flowers is illustrated in Scheme 1. In the initial stage, $Co(OH)_2$ colloids are produced and aggregated to solid microspheres to decrease the surface energy (Step 1). Over the course of the reaction the concentration of the reactants in the surrounding solution decrease so that supersaturation falls over time and a chemical equilibrium between the solid-liquid interfaces is established. Meanwhile, the smaller interior crystallites are still in nonequilibrium state. In this process, the exterior crystallites will serve as starting points to attract the smaller metastable crystallites underneath the surface layer. These smaller crystallites that remain out of the equilibrium with the surrounding solution are easily dissolved and diffused outwards. As a consequence, the supersaturation increases above the solubility product of the exterior layer in the solution which results in secondary deposition of inorganic products on the exterior surface and divides the solid spheres into two discrete regions to form a core-shell structure. Owing to the flakelike growth habit of β-$Co(OH)_2$, the new deposition process results in surface nanoflakes (Step 2). The void space between the outer shell and the inner core will be enlarged and the core region will be trimmed down to smaller size because of the gradual mass diffusion when a longer reaction time is applied (Step 3). In the final stage, the inner core is completely consumed through this dissolution-recrystallization process (Step 4 and 5), in the meanwhile the sphere size increases perceptibly, as the core dissolves progressively to produce a hollow structure. In particular, the increase of crystallinity and the growth of crystal size with the reaction time can also indicate that Ostwald ripening is an underlying mechanism in this hollowing process.

In this system, reaction temperature is proposed to be not a crucial parameter affecting product morphology and composition. Its effect on product is just to change the ripening rate of this flowerlike product. With a constant reaction system same as Sample 1, if the temperature was decreased to 180 °C (Sample 7), as shown in Figure 7a, we got a flowerlike core-shell product that matches Sample 6, which was obtained at 200 °C after 4 h. If the reaction temperature was raised to 220 °C, flowerlike hollow spheres with a diameter of about 5 μm were obtained (Sample 8, Figure 7b). The surface of the hollow spheres consisted of radially prickly nanoflakes, the same as the product obtained at 200 °C after 15 h. Thus, it can be confirmed that, if maintaining a constant reaction system, the reaction temperature can control the ripening rate, the higher the temperature the faster the rate.

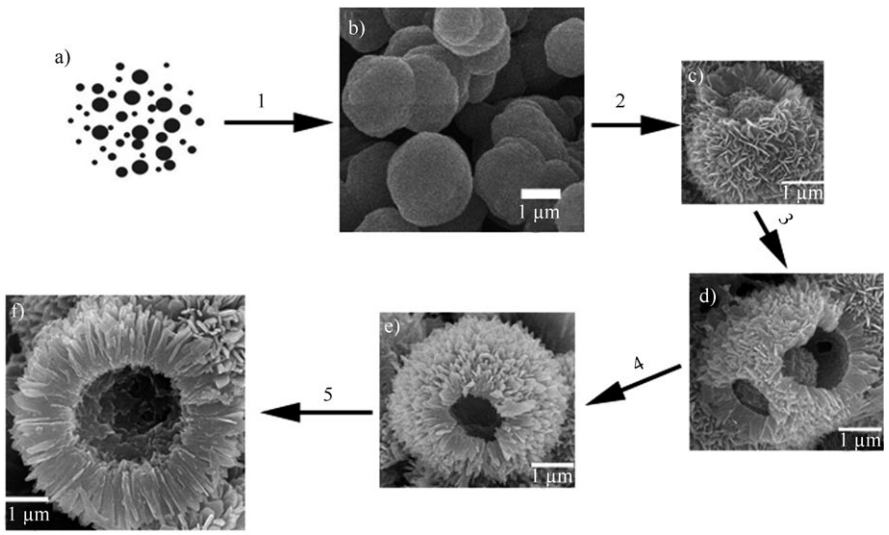

Scheme 1. Schematic illustration of the formation of β-$Co(OH)_2$ hollow flowers through the Ostwald ripening process. The $Co(OH)_2$ samples at different growth stages were prepared for b) 3 h, c) 4 h, d) 6 h, e) 8 h, and f) 15 h, respectively.

Metallic cobalt is obtained by thermal conversion of the β-$Co(OH)_2$ flower precursor. The XRD pattern of residual product obtained following heating at 400 °C for 2 h in Ar is shown in Figure 8a. A mixture of Co (JCPDS file no. 89-4308) and CoO (JCPDS file no. 75-0393) is formed and reveals that a redox reaction has taken place. We propose that this process is caused by thermal decomposition of ethylene glycol. Ethylene glycol is a neutral solvent with two -OH bonds and is generally referred to be a capping agent. Therefore, it can be

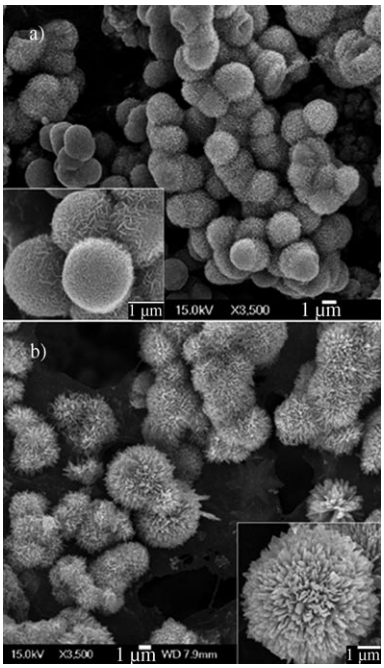

Figure 7. a,b) (insets) FESEM images of flowerlike β-$Co(OH)_2$ products obtained from Sample 7 and Sample 8 by changing reaction temperature to 180° and 220°, respectively.

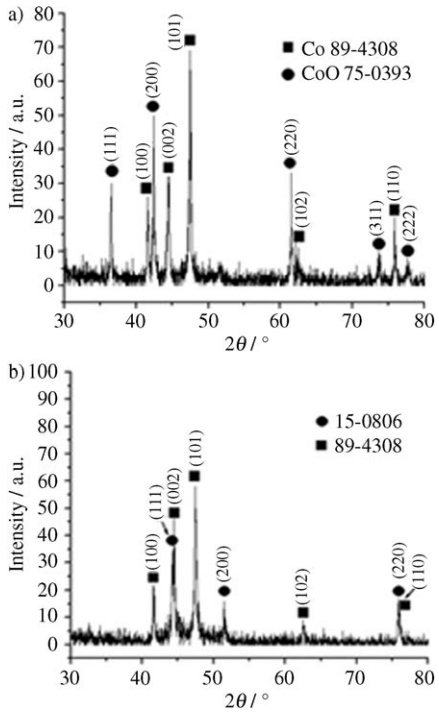

Figure 8. a,b) XRD patterns of decomposed residues of cobalt hydroxide flower precursor obtained following heating in Ar and in mixed gas of Ar+4% H_2, respectively.

linked on the surface of $Co(OH)_2$ crystallites. This capping material can be decomposed thermally by a calcination at high temperature, which results in the reduction of a part of Co^{2+} to Co^0. The other parts were converted into cobalt oxide. If this calcination process is carried out in a mixed gas of Ar+4% of H_2, we can get metallic Co residue with two different crystal structure, cubic (JCPDS file no. 15–0806) and hexagonal (JCPDS file no. 89–4308) (Figure 8b). The FESEM image in Figure 9 shows the spherical morphology of Co, and the high-magnification image (inset of Figure 9a) indicates that these products have preserved the hollow core structure. The shell consists of Co nanoparticles and amorphous wirelike nanostructures, which should be the residue of decomposed organic compounds (Figure 9b,c, SAED data not shown). The existence of oxygen in the EDS analysis was a result of oxidation by air.

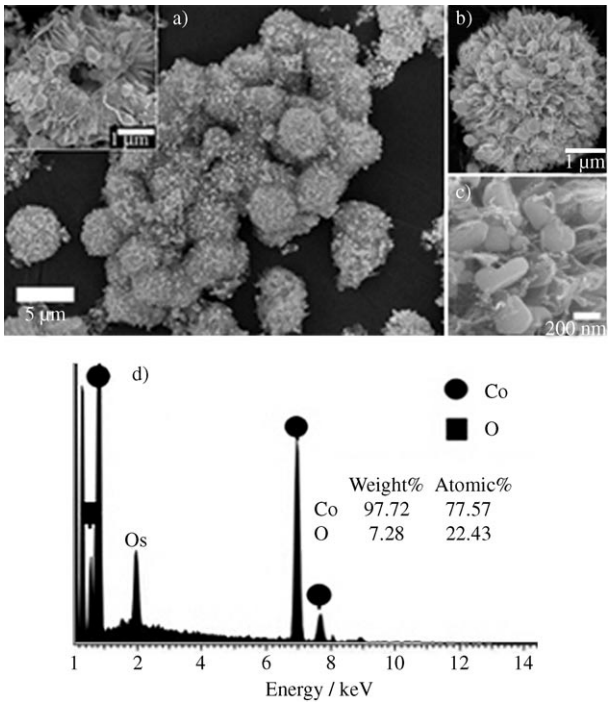

Figure 9. a–c) (inset) FESEM images of metallic Co hollow spheres obtained by thermal conversion of β-$Co(OH)_2$ flower precursor in mixed gas of Ar and 4% H_2. d) EDS spectrum of Co hollow spheres.

Conclusion

In summary, we have presented a high-yield synthesis of flowerlike hollow spheres of β-$Co(OH)_2$ through a selected-control solvothermal route for the first time. Although hollow spheres have been previously been prepared by two main preparative categories: 1) template-directed synthesis and 2) emulsion synthesis,[15] the approach described herein based on the morphologically confined process of Ostwald ripening could be significant in terms of the ease of preparation and the cost of these process. In addition, cobalt hollow spheres were correspondingly obtained by thermal decomposition of $Co(OH)_2$ flower precursors through the redox reaction caused by decomposition of organic compounds and the presence of 4% of H_2. Potentially, the superpara-

magnetic behavior of Co allows these hollow spheres to be used as directed materials in biotechnology.

Experimental Section

Materials preparation: All chemical reagents were of analytical grade and used as received without purification. In a typical procedure, $CoCl_2 \cdot 6H_2O$ (2 mmol), and NaOH (2.5 mmol) were dissolved in mixed solvent of ethylene glycol (40 mL) and distilled water (from 0.1 mL to 10 mL) under vigorous stirring to form a homogeneous solution. The solution was quickly transferred into a stainless steel autoclave with a Teflon liner of 60 mL capacity, and heated in an oven at 200 °C (180 °C or 220 °C) for different reaction times ranging from 1.5 to 15 h. After the autoclave was air-cooled to room temperature, the resulting pink precipitates were collected by centrifugation. By washing with anhydrous ethanol for several times, the pink powders then were dried in a vacuum at 60 °C for further characterization. Table 1 summarizes the synthesis parameters for the samples.

Metallic cobalt hollow spheres were obtained by thermal decomposition of flowerlike cobalt hydroxide hollow spheres in a mixed gas of Ar+4 % H_2. Cobalt hydroxide was heated to 400 °C for 2 h at a heating rate of 3 °C min^{-1}, and then cooled to room temperature. The gray-black product was collected for the following characterization.

Characterization: The XRD patterns of the synthesized cobalt hydroxide samples were characterized by using an X-ray diffractometer (X′Pert-MPD, Philips) with $Cu_{K\alpha}$ radiation. The microstructures and compositional information of the samples were studied by using a field-emission scanning electron microscope with energy-dispersive X-ray spectroscopy (FESEM/EDS, JEOL JSM-6700F), transmission electron microscope (TEM, HITACHI, H-7500), and high-resolution transmission electron microscope and the corresponding selected area electron diffraction (HRTEM/SAED, JEOL JEM-2010).

Acknowledgement

This work is financially supported by the Korea Research Foundation Grant No. KRF-2006-211-C00013 and Brain Korea 21 program.

[1] W. Li, S. Zhang, J. Chen, *J. Phys. Chem. B* **2005**, *109*, 14025–14032.
[2] L. Cao, F. Xu, Y.-Y. Liang, H.-L. Li, *Adv. Mater.* **2004**, *16*, 1853–1857.
[3] a) M. Vidotti, M. R. Silva, R. P. Salvador, S. I. Córdoba de Torresi, L. H. Dall′Antonia, *Electrochim. Acta* **2008**, *53*, 4030–4034; b) M. Jafarian, M. G. Mahjani, H. Heli, F. Gobal, H. Khajehsharifi, M. H. Hamedi, *Electrochim. Acta* **2003**, *48*, 3423–3429.
[4] M. Kurmoo, *Chem. Mater.* **1999**, *11*, 3370–3378.
[5] M. S. Yarger, E. M. P. Steinmiller, K.-S. Choi, *Chem. Commun.* **2007**, 159–161.
[6] R. Ma, Z. Liu, K. Takada, K. Fukuda, Y. Ebina, Y. Bando, T. Sasaki, *Inorg. Chem.* **2006**, *45*, 3964–3969.
[7] a) Z. Liu, R. Ma, M. Osada, K. Takada, T. Sasaki, *J. Am. Chem. Soc.* **2005**, *127*, 13869–13874; b) Y. Zhu, H. Li, Y. Koltypin, A. Gedanken, *J. Mater. Chem.* **2002**, *12*, 729–733; c) Y. Oaki, H. Imai, *J. Mater. Chem.* **2007**, *17*, 316–321; d) R. S. Jayashree, P. V. Kamath, *J. Mater. Chem.* **1999**, *9*, 961–963; e) Y. Hou, H. Kondoh, M. Shimojo, T. Kogure, T. Ohta, *J. Phys. Chem. B* **2005**, *109*, 19094–19098; f) L. Poul, N. Jouini, F. Fiévet, *Chem. Mater.* **2000**, *12*, 3123–3132; g) J. T. Sampanthar, H. C. Zeng, *J. Am. Chem. Soc.* **2002**, *124*, 6668–6675.
[8] L. Zhang, A. K. Dutta, G. Jarero, P. Stroeve, *Langmuir* **2000**, *16*, 7095–7100.
[9] a) R. Xu, H. C. Zeng, *J. Phys. Chem. B.* **2003**, *107*, 12643–12649; b) E. Hosono, S. Fujihara, I. Honma, H. Zhou, *J. Mater. Chem.* **2005**, *15*, 1938–1945.
[10] a) X. W. Lou, D. Deng, J. Y. Lee, J. Feng, L. A. Archer, *Adv. Mater.* **2008**, *20*, 258–262; b) P. Jeevanandam, Y. Koltypin, A. Genanken, Y. Mastai, *J. Mater. Chem.* **2000**, *10*, 511–514.
[11] B. Li, Y. Xie, C. Wu, Z. Li, J. Zhang, *Mater. Chem. Phys.* **2006**, *99*, 479–486.
[12] L.-X. Yang, Y.-J. Zhu, L. Li, L. Zhang, H. Tong, W.-W. Wang, G.-F. Cheng, J.-F. Zhu, *Eur. J. Inorg. Chem.* **2006**, *2006*, 4787–4792.
[13] a) W. Z. Ostwald, *Phys. Chem.* **1900**, *34*, 495–503; b) H. G. Yang, H. C. Zeng, *Angew. Chem.* **2004**, *116*, 5318–5321; *Angew. Chem. Int. Ed.* **2004**, *43*, 5206–5209; c) B. Liu, H. C. Zeng, *Small* **2005**, *1*, 566–571; d) R. Qiao, X. L. Zhang, R. Qiu, J. C. Kim, Y. S. Kang, *Chem. Mater.* **2007**, *19*, 6485–6491; e) J. Yu, H. Guo, S. A. Davis, S. Mann, *Adv. Funct. Mater.* **2006**, *16*, 2035–2041; f) J. Yu, H. Yu, H. Guo, M. Li, S. Mann, *Small* **2008**, *4*, 87–91.
[14] H. Li, Z. Bian, J. Zhu, D. Zhang, G. Li, Y. Huo, H. Li, Y. Lu, *J. Am. Chem. Soc.* **2007**, *129*, 8406–8407.
[15] a) F. Caruso, R. A. Caruso, H. Möhwald, *Science* **1998**, *282*, 1111–1114; b) N. A. Dhas, K. S. Suslick, *J. Am. Chem. Soc.* **2005**, *127*, 2368–2369; c) M. Chen, L. M. Wu, S. X. Zhou, B. You, *Adv. Mater.* **2006**, *18*, 801–806; d) P. Wang, D. Chen, F. Q. Tang, *Langmuir* **2006**, *22*, 4832–4835; e) Z. Yang, Z. Niu, Y. Lu, Z. Hu, C. C. Han, *Angew. Chem.* **2003**, *115*, 1987–1989; *Angew. Chem. Int. Ed.* **2003**, *42*, 1943–1945; f) Q. Y. Sun, P. J. Kooyman, J. G. Grossmann, P. H. H. Bomans, P. M. Frederik, P. C. M. M. Magusin, T. P. M. Beelen, R. A. V. Santen, N. A. J. M. Sommerdijk, *Adv. Mater.* **2003**, *15*, 1097–1100.

Received: April 28, 2008
Published online: January 8, 2009

